

## Geological Society of America Special Papers Online First

### Site response in the eastern United States: A comparison of Vs30 measurements with estimates from horizontal:vertical spectral ratios

Daniel E. McNamara, William J. Stephenson, Jack K. Odum, et al.

*Geological Society of America Special Papers*, published online September 30, 2014;  
doi:10.1130/2015.2509(04)

---

**E-mail alerting services** click [www.gsapubs.org/cgi/alerts](http://www.gsapubs.org/cgi/alerts) to receive free e-mail alerts when new articles cite this article

**Subscribe** click [www.gsapubs.org/subscriptions](http://www.gsapubs.org/subscriptions) to subscribe to Geological Society of America Special Papers

**Permission request** click [www.geosociety.org/pubs/copyrt.htm#gsa](http://www.geosociety.org/pubs/copyrt.htm#gsa) to contact GSA.

Copyright not claimed on content prepared wholly by U.S. government employees within scope of their employment. Individual scientists are hereby granted permission, without fees or further requests to GSA, to use a single figure, a single table, and/or a brief paragraph of text in subsequent works and to make unlimited copies of items in GSA's journals for noncommercial use in classrooms to further education and science. This file may not be posted to any Web site, but authors may post the abstracts only of their articles on their own or their organization's Web site providing the posting includes a reference to the article's full citation. GSA provides this and other forums for the presentation of diverse opinions and positions by scientists worldwide, regardless of their race, citizenship, gender, religion, or political viewpoint. Opinions presented in this publication do not reflect official positions of the Society.

---

Notes

The Geological Society of America  
Special Paper 509  
2015

*Site response in the eastern United States:  
A comparison of Vs30 measurements with  
estimates from horizontal:vertical spectral ratios*

Daniel E. McNamara  
William J. Stephenson  
Jack K. Odum  
Robert A. Williams

*U.S. Geological Survey, Geologic Hazards Science Center, 1711 Illinois St., Golden, Colorado 80401, USA*

Lind Gee

*U.S. Geological Survey, Albuquerque Seismological Laboratory, PO Box 82010, Albuquerque, New Mexico 87198-2010, USA*

ABSTRACT

Earthquake damage is often increased due to local ground-motion amplification caused by soft soils, thick basin sediments, topographic effects, and liquefaction. A critical factor contributing to the assessment of seismic hazard is detailed information on local site response. In order to address and quantify the site response at seismograph stations in the eastern United States, we investigate the regional spatial variation of horizontal:vertical spectral ratios (HVSR) using ambient noise recorded at permanent regional and national network stations as well as temporary seismic stations deployed in order to record aftershocks of the 2011 Mineral, Virginia, earthquake. We compare the HVSR peak frequency to surface measurements of the shear-wave seismic velocity to 30 m depth ( $V_{s30}$ ) at 21 seismograph stations in the eastern United States and find that HVSR peak frequency increases with increasing  $V_{s30}$ . We use this relationship to estimate the National Earthquake Hazards Reduction Program soil class at 218 ANSS (Advanced National Seismic System), GSN (Global Seismographic Network), and RSN (Regional Seismograph Networks) locations in the eastern United States, and suggest that this seismic station-based HVSR proxy could potentially be used to calibrate other site response characterization methods commonly used to estimate shaking hazard.

## INTRODUCTION

The estimation of the earthquake hazard at a site depends on many factors, including the distribution of the seismic source zones, the return times of large events, the predominant earthquake mechanisms near each site, the path effects of the transmitting medium (the Earth), and local site effects on the seismic waves. Local site amplification for a single earthquake can vary significantly due to the presence of soft soils (Martin, 1994), thick basin sediments (Mundepi et al., 2009; Odum et al., 2010; Bodin and Horton, 1999; Pratt and Brocher, 2006), and topography (Toshinawa et al., 2004; Hartzell et al., 2014). Constraining the spatial variability of local site amplification is important in order to improve ground-motion prediction equations used to develop the U.S. Geological Survey (USGS) national seismic hazard map (Petersen et al., 2008) and determine seismic provisions in building codes in the United States (Building Seismic Safety Council, 2009).

Compared to the western United States, earthquakes in the eastern United States are less frequent but typically felt, and cause damage over a much broader region due to efficient energy propagation (low attenuation) through the crystalline bedrock that underlies much of the eastern United States (Frankel et al., 1996; Benz et al., 1997). Although they are relatively infrequent, the eastern United States has experienced numerous earthquakes during historical time that have caused significant damage from ground shaking. Most recently, a moment magnitude ( $M_w$ ) 5.8 earthquake occurred on 23 August 2011 (17:51:04 UTC, Coordinated Universal Time) near Mineral, Virginia (Fig. 1) (McNamara et al., 2014a; Chapman, 2013). The earthquake ruptured a southeast-dipping northeast-striking reverse fault within a region of diffuse seismicity known as the Central Virginia seismic zone (CVSZ) (Chapman, 2005; Algermissen and Perkins, 1976; Bollinger, 1969).

Ground shaking associated with the 2011 Mineral earthquake was felt (Modified Mercalli Intensity,  $MMI \geq II$ ) over a large region due to the relatively low attenuation (high  $Q$ ) properties of the crust in the eastern United States (McNamara et al., 2014b). An estimated 10,000 people were exposed to moderate to heavy shaking levels ( $MMI = VIII$ ) and 23,000 were exposed to  $MMI = VI$ , according to the USGS PAGER (Prompt Assessment of Global Earthquakes for Response) system (Wald et al., 2010; [earthquake.usgs.gov/earthquakes/pager](http://earthquake.usgs.gov/earthquakes/pager)). Postearthquake damage assessments found that moderately heavy damage ( $MMI = VII-VIII$ ) occurred to single and multistory homes and buildings in a rural area of Louisa County, southwest of Mineral (Li, 2013; Earthquake Engineering Research Institute Special Earthquake Report, 2011) (Fig. 1A). In McNamara et al. (2014b) we showed that the contributions of both azimuthally dependent attenuation ( $1/Q$ ) and local site amplification are required to explain the regional distribution of intensity observations, as well as the locally high shaking intensity observations ( $MMI V-VII$ ) in specific areas such as Washington, D.C., and coastal zones of the northeastern United States (Hough, 2012).

Multiple organizations deployed portable seismic stations in the days after the Mineral earthquake in order to record aftershocks (McNamara et al., 2014a). The combined seismic network that includes the permanent USGS Advanced National Seismic System (ANSS), EarthScope Transportable Array (TA), Regional Seismic Networks (RSN), and temporary portable seismic stations makes this aftershock sequence one of the best-recorded in the eastern United States (Fig. 1; Table 1). The abundance of aftershocks and local seismic stations presents new opportunities to better quantify eastern United States ground-shaking parameters.

Given the recent emphasis on understanding earthquake hazards in the eastern United States following the 2011 Mineral earthquake, Vs30 (shear-wave seismic velocity to 30 m depth) was measured at 66 portable and permanent seismic station locations in the CVSZ and greater eastern U.S. region (Electric Power Research Institute, 2012; Stephenson et al., this volume; R. Kayen, 2012, written commun.). Based on numerous empirical studies (Borcherdt and Gibbs, 1976; Borcherdt, 1994; Wills and Silva, 1998), Vs30 has become the most common means of classifying site conditions (soil class) and has been adopted in the National Earthquake Hazard Reduction Program (NEHRP) design provisions for new buildings (Martin, 1994). Because surface Vs30 measurements are sparse, proxy methods are often used to estimate Vs30 and soil class at most locations for USGS earthquake assessment and hazard products such as Shakemap and the national seismic hazard map.

In this paper we investigate the potential for horizontal:vertical spectral ratios (HVSR) of ambient noise as a proxy for Vs30 estimates. We compute HVSR using ambient noise signal recorded at permanent and portable seismic stations in the eastern United States (Fig. 1). We show a clear relationship between HVSR peak frequency and Vs30 measured on the ground surface near seismic stations in the CVSZ (Electric Power Research Institute, 2012; Stephenson et al., this volume; R. Kayen, 2012, personal commun.). We then assume the CVSZ regional relationship between HVSR peak frequency and surface measurements of Vs30 in order to estimate Vs30 and soil class at 218 permanent seismic stations in the eastern United States. We suggest that this HVSR proxy could be used to calibrate topographic slope estimates of Vs30 that are commonly used to estimate shaking hazard.

## HVSR METHODS AND RESULTS

The premise of the HVSR method is that in shallow sedimentary deposits differences in the shear-wave impedance contrasts are larger than compressional-wave impedance changes. The underlying assumption is that when shear waves impinge on the boundary between bedrock and shallow sedimentary deposits, vertical shear (SV) waves will convert to primary (P) waves and pass through the overlying layer relatively unaltered, while the horizontal shear (SH) waves will be strongly influenced by sedimentary layers (Nakamura, 1989). HVSR is generally

Comparison of Vs30 measurements with estimates from horizontal:vertical spectral ratios

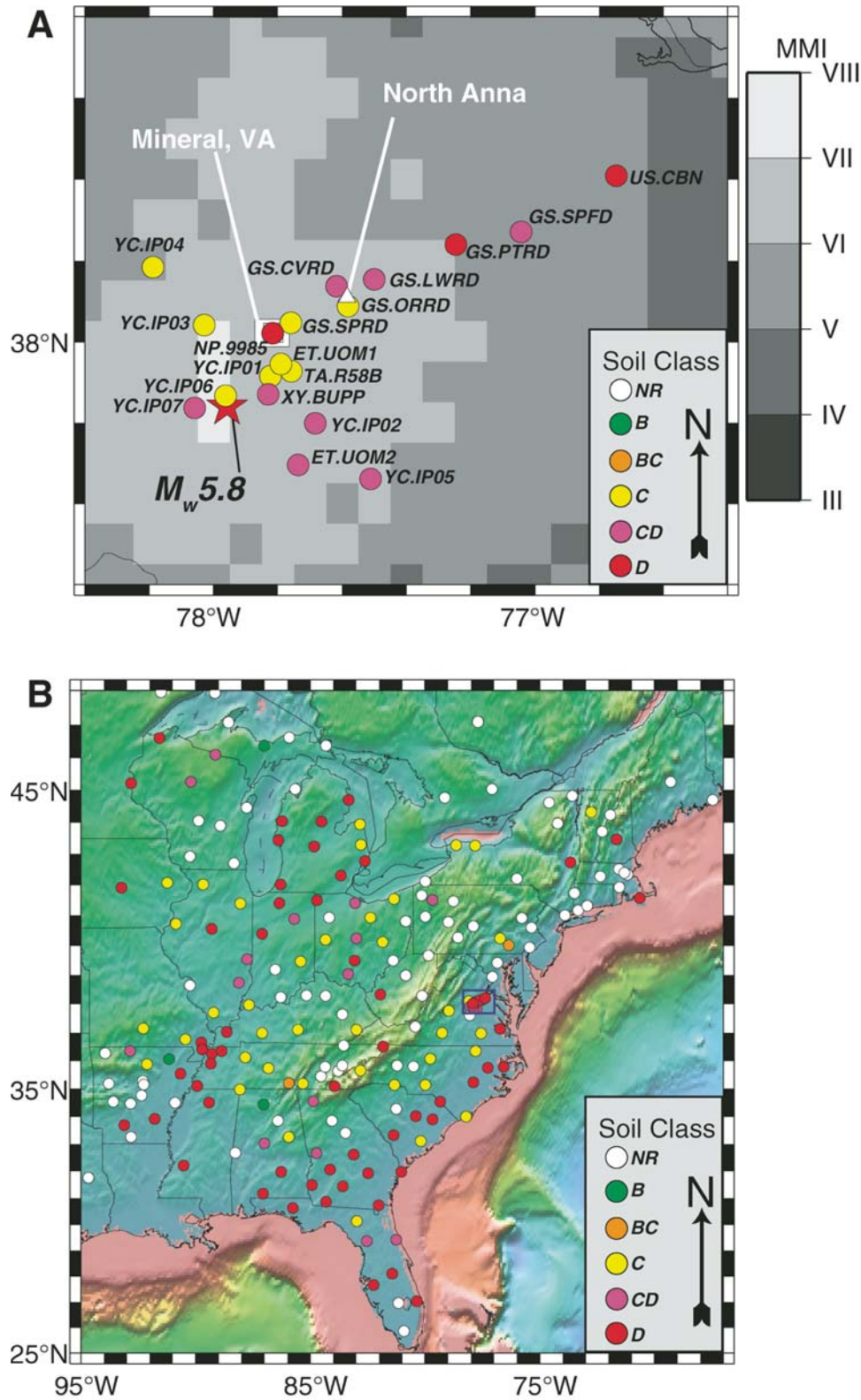


Figure 1. Map of seismic stations used in this study. (A) Map of the Mineral, Virginia, epicentral region showing Modified Mercalli Intensity (MMI) from the 2011  $M_w$  5.8 earthquake and soil classes for stations determined in this study. The location of the Mineral earthquake (red star) is from McNamara et al. (2014a). The location of the North Anna nuclear power plant is shown as a white triangle. (B) Map of 218 permanent and portable seismic stations in the eastern United States at which this study estimated National Earthquake Hazard Reduction Program soil class (Table 1). NR—no results.

McNamara *et al.*

TABLE 1. SOIL CHARACTERISTICS AT 218 SEISMIC STATIONS IN THE EASTERN UNITED STATES

Net.Station	HVSR peak frequency (Hz)	HVSR Vs30 (m/s)	NEHRP Soil Class
AG.CCAR	0.65	288.3	D
AG.FCAR	5.0	513.7	C
AG.HHAR	NR	NR	NR
AG.LCAR	20	1290.7	B
AG.WHAR	NR	NR	NR
AG.WLAR	0.35	272.8	D
CN.PLVO	NR	NR	NR
CN.SADO	NR	NR	NR
CO.JSC	NR	NR	NR
ET.CPCT	NR	NR	NR
ET.SWET	10.0	772.7	BC
GS.CVRD	2.5	384.2	CD
GS.LWRD	2.25	371.2	CD
GS.ORRD	8.0	669.1	C
GS.PTRD	1.5	332.4	D
GS.SPFD	3.0	410.1	CD
GS.SPRD	4.0	461.9	C
IM.TKL	NR	NR	NR
IU.DWPF	1.4	327.2	D
IU.HRV	NR	NR	NR
IU.SSPA	NR	NR	NR
IU.WCI	NR	NR	NR
IU.WVT	8.5	695	C
LD.ALLY	NR	NR	NR
LD.FRNY	NR	NR	NR
LD.KSCT	NR	NR	NR
LD.LUPA	NR	NR	NR
LD.MVL	10	772.7	BC
LD.NCB	NR	NR	NR
LD.PAL	NR	NR	NR
LD.SDMD	NR	NR	NR
NE.BCX	NR	NR	NR
NE.BRYW	NR	NR	NR
NE.EMMW	NR	NR	NR
NE.FFD	1.5	332.4	D
NE.HNH	NR	NR	NR
NE.QUA2	NR	NR	NR
NE.TRY	0.5	280.6	D
NE.VT1	3.5	436	C
NE.WES	NR	NR	NR
NE.WSPT	NR	NR	NR
NE.YLE	NR	NR	NR
NM.BLO	NR	NR	NR
NM.GLAT	0.2	265.0	D
NM.HALT	0.25	267.6	D
NM.HBAR	0.25	267.6	D
NM.MGMO	8.0	669.1	C
NM.MPH	0.18	264.0	D
NM.OLIL	2.5	384.2	CD
NM.PARM	0.4	275.4	D
NM.PBMO	3.5	436	C
NM.PLAL	3.5	436	C
NM.PVMO	0.25	267.6	D
NM.SLM	NR	NR	NR
NM.UALR	NR	NR	NR
NM.USIN	9.0	720.9	C
NM.UTMT	0.35	272.83	D

(Continued)

TABLE 1. SOIL CHARACTERISTICS AT 218 SEISMIC STATIONS IN THE EASTERN UNITED STATES (Continued)

Net.Station	HVSR peak frequency (Hz)	HVSR Vs30 (m/s)	NEHRP Soil Class
NP.9985	1.6	337.58	D
NQ.WNC	NR	NR	NR
PE.NCAT	4.5	487.8	C
PE.PAGS	5.0	513.7	C
PE.PSUB	NR	NR	NR
TA.059A	NR	NR	NR
TA.060A	0.45	278.01	D
TA.061Z	NR	NR	NR
TA.147A	NR	NR	NR
TA.152A	2.5	384.2	CD
TA.154A	0.3	270.24	D
TA.250A	0.25	267.65	D
TA.253A	0.9	301.32	D
TA.255A	1.1	311.68	D
TA.257A	1.5	332.4	D
TA.352A	1.0	306.5	D
TA.451A	2.0	358.3	D
TA.453A	1.5	332.4	D
TA.456A	1.0	306.5	D
TA.555A	4.0	461.9	C
TA.656A	3.0	410.1	CD
TA.658A	2.2	368.66	CD
TA.957A	1.5	332.4	D
TA.C40A	NR	NR	NR
TA.D41A	NR	NR	NR
TA.D53A	NR	NR	NR
TA.E38A	2.0	358.3	D
TA.E43A	11	824.5	B
TA.E44A	NR	NR	NR
TA.E46A	NR	NR	NR
TA.G40A	2.5	384.2	CD
TA.G45A	NR	NR	NR
TA.H43A	NR	NR	NR
TA.H48A	1.0	306.5	D
TA.I41A	NR	NR	NR
TA.I42A	NR	NR	NR
TA.I45A	0.7	290.9	D
TA.I47A	1.5	332.4	D
TA.I49A	6.0	565.5	C
TA.J45A	0.8	296.1	D
TA.J47A	1.2	316.8	D
TA.J48A	4.5	487.8	C
TA.J54A	3.9	456.7	C
TA.J55A	5.5	539.6	C
TA.K43A	NR	NR	NR
TA.K50A	1.5	332.4	D
TA.KMSC	4.0	461.9	C
TA.L40A	6.5	591.4	C
TA.L42A	5.5	539.6	C
TA.L46A	1.2	316.8	D
TA.M44A	6.0	565.5	C
TA.M46A	1.4	327.2	D
TA.M48A	1.3	322.0	D
TA.M50A	2.5	384.2	CD
TA.M52A	5.5	539.6	C
TA.M54A	2.5	384.2	CD
TA.M55A	NR	NR	NR

(Continued)

## Comparison of Vs30 measurements with estimates from horizontal:vertical spectral ratios

TABLE 1. SOIL CHARACTERISTICS AT 218 SEISMIC STATIONS IN THE EASTERN UNITED STATES (*Continued*)

Net.Station	HVSR peak frequency (Hz)	HVSR Vs30 (m/s)	NEHRP Soil Class
TA.M65A	0.85	298.7	D
TA.N41A	5.5	539.6	C
TA.N47A	2.5	384.2	CD
TA.N49A	NR	NR	NR
TA.N51A	4.0	461.9	C
TA.N53A	NR	NR	NR
TA.N54A	NR	NR	NR
TA.N55A	NR	NR	NR
TA.N59A	NR	NR	NR
TA.O49A	6.0	565.5	C
TA.O52A	4.5	487.8	C
TA.O56A	NR	NR	NR
TA.P45A	3.0	410.1	CD
TA.P48A	4.2	472.2	C
TA.P51A	1.5	332.4	D
TA.P53A	NR	NR	NR
TA.Q51A	3.0	410.1	CD
TA.Q54A	NR	NR	NR
TA.R49A	NR	NR	NR
TA.R50A	NR	NR	NR
TA.R53A	2.0	358.3	D
TA.R55A	NR	NR	NR
TA.R58B	3.5	436	C
TA.S51A	NR	NR	NR
TA.S57A	3.5	436	C
TA.S58A	NR	NR	NR
TA.SFIN	0.9	301.32	D
TA.SPMN	2.0	358.3	D
TA.T45A	0.75	293.5	D
TA.T47A	6.5	591.4	C
TA.T49A	3.5	436	C
TA.T52A	8.0	669.1	C
TA.T57A	3.8	451.54	C
TA.T59A	7.0	617.3	C
TA.T60A	0.35	272.83	D
TA.TIGA	1.5	332.4	D
TA.TUL1	NR	NR	NR
TA.U40A	2.5	384.2	CD
TA.U54A	1.5	332.4	D
TA.U59A	2.1	363.4	C
TA.V48A	7.0	617.3	C
TA.V51A	NR	NR	NR
TA.V52A	NR	NR	NR
TA.V53A	6.0	565.5	C
TA.V55A	NR	NR	NR
TA.V56A	NR	NR	NR
TA.V60A	0.6	285.7	D
TA.V61A	0.2	265.0	D
TA.W39A	NR	NR	NR
TA.W41B	NR	NR	NR
TA.W50A	7.8	658.7	C
TA.W52A	1.9	353.1	D
TA.W57A	4.5	487.8	C
TA.WHTX	NR	NR	NR
TA.X40A	NR	NR	NR
TA.X43A	NR	NR	NR
TA.X48A	11	824.5	B

*(Continued)*TABLE 1. SOIL CHARACTERISTICS AT 218 SEISMIC STATIONS IN THE EASTERN UNITED STATES (*Continued*)

Net.Station	HVSR peak frequency (Hz)	HVSR Vs30 (m/s)	NEHRP Soil Class
TA.X51A	3.0	410.1	CD
TA.X58A	0.8	296.1	D
TA.Y49A	NR	NR	NR
TA.Y52A	NR	NR	NR
TA.Y57A	1.1	311.6	D
TA.Y58A	0.4	275.4	D
TA.Y60A	4.0	461.9	C
TA.Z41A	NR	NR	NR
TA.Z50A	3.2	420.4	C
TA.Z56A	0.5	280.6	D
US.AAM	1.4	327.2	D
US.ACSO	3.0	410.1	CD
US.AGMN	1.5	332.4	D
US.BINY	NR	NR	NR
US.BLA	NR	NR	NR
US.BRAL	1.4	327.2	D
US.CBN	0.7	290.9	D
US.CNNC	0.9	301.3	D
US.COWI	2.4	379.0	CD
US.ERPA	NR	NR	NR
US.EYMN	NR	NR	NR
US.GOGA	NR	NR	NR
US.HDIL	0.9	301.3	D
US.JFWS	NR	NR	NR
US.LBNH	NR	NR	NR
US.LONY	NR	NR	NR
US.LRAL	2.5	384.2	CD
US.MCWV	NR	NR	NR
US.MIAR	NR	NR	NR
US.NATX	NR	NR	NR
US.NHSC	4.5	487.8	C
US.OXF	0.4	275.4	D
US.PKME	NR	NR	NR
US.SCIA	1.1	311.6	D
US.TZTN	NR	NR	NR
US.VBMS	1.7	342.7	D
YC.IP01	4.5	487.8	C
YC.IP02	2.5	384.2	CD
YC.IP03	4.0	461.9	C
YC.IP04	4.0	461.9	C
YC.IP05	2.75	397.1	CD
YC.IP06	5.0	513.7	C
YC.IP07	2.3	373.8	CD
ET.UOM1	9.0	720.9	C
ET.UOM2	2.5	384.2	CD
XY.BUPP	2.7	394.5	CD
NM.SIUC	5.5	539.6	C

*Note:* HVSR—horizontal:vertical spectral ratios; Vs30—shear-wave velocity to a depth of 30 m; NEHRP—National Earthquake Hazard Reduction Program. NR—no result (i.e., stations with no clear HVSR peak).

considered to be a reliable measure of the primary resonance frequency but not to accurately determine local site amplification (Edwards *et al.*, 2013; Pratt and Brocher, 2006; Field and Jacob, 1995). Primary resonance frequency is an important parameter to determine because resonance may increase or amplify a building's response to ground shaking, especially if ground motions are at frequencies close or equal to the natural resonant frequency of the structure.

We use the spectral analysis system PQLX (Passcal Quick Look Extended; McNamara and Boaz, 2010) to compute all spectra used in our HVSR analysis. In this approach, the variation of spectral power is observed by computing instrument-corrected power spectral density (PSD) probability density functions (PDFs) after the methods in McNamara and Buland (2004). Percentile statistics derived from the PSD PDFs are used to estimate a smoothed distribution of spectral power as a function of frequency for each component of motion and to form the HVSR estimates.

In order to obtain the maximum number of possible HVSR estimates in the eastern United States, we use seismic stations equipped with instrumentation that records either weak or strong ground motion; however, each requires different processing steps. For our HVSR analysis using weak-motion seismic stations, we are interested in isolating the ambient noise spectra from spectral transients due to earthquakes and recording system problems. We use the long-term PSD PDFs to isolate the ambient noise spectra by trimming hourly PSDs that are outside of the 5th and 90th percentiles of the PDF. Figure 2 shows long-term PSD PDFs for weak-motion channels from the USGS portable aftershock station GS.SPFD (Fig. 1; Table 1). The horizontal channel (BHE) PSD PDF shown in Figure 2A is constructed using 11,941 PSDs computed from hourly time segments overlapping by 50% that range from 28 August 2011 through 21 March 2012. Figure 2B shows the vertical channel (BHZ) long-term PSD PDF computed using 11,939 PSDs during the same time range. The long-term PSD PDF median (50%) spectra that is derived from weak-

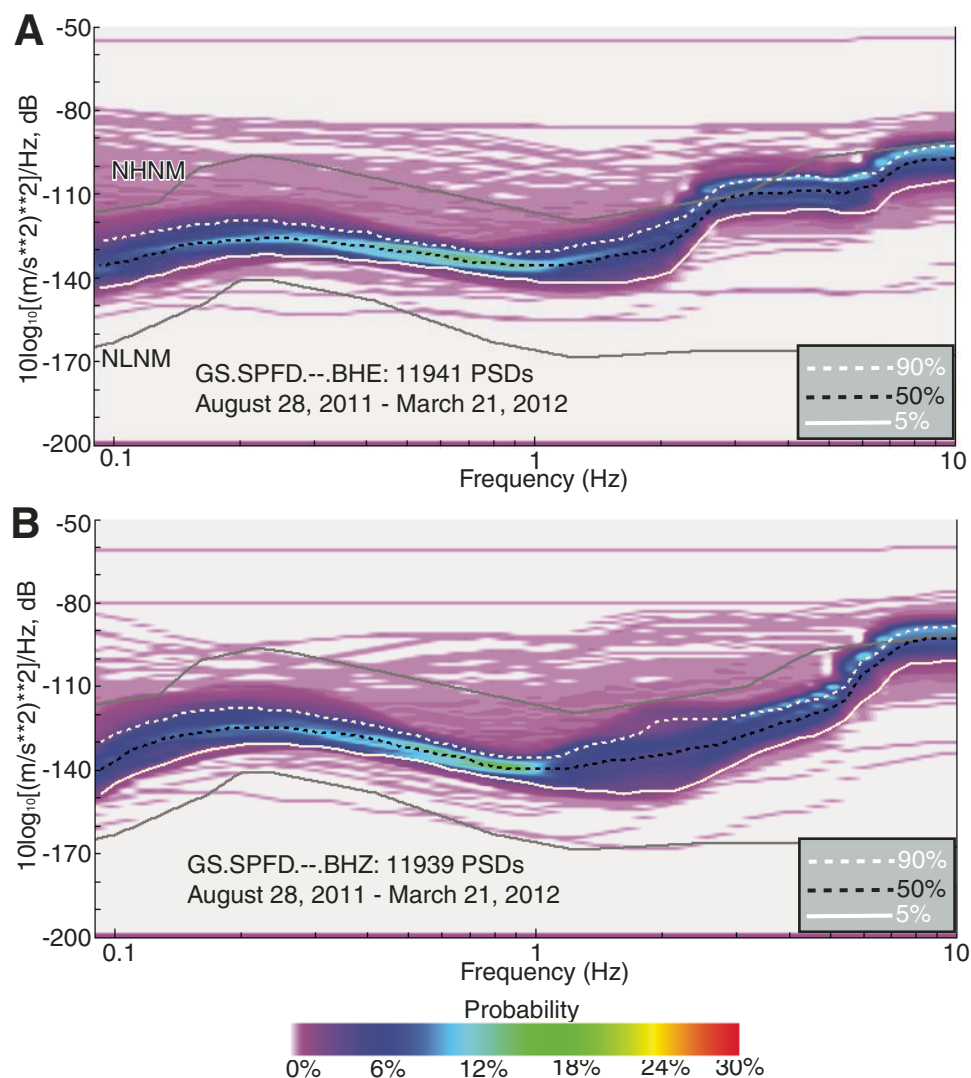


Figure 2. Power spectral density (PSD) probability density functions (PDFs) computed for two-components of weak motion (broadband) recordings by portable aftershock station GS.SPFD. Black dashed lines—long-term PSD PDF medians (50%); white lines show additional percentiles. Gray lines NHHM, NLNM are new high and low noise models (from Peterson, 1993). (A) PDF formed from 11941 PSDs recorded from 28 August 2011 through 21 March 2012 on channel GS.SPFD--.BHE. (B) PDF formed from 11939 PSDs from channel GS.SPFD--.BHZ. Double asterisks represent exponent.

## Comparison of Vs30 measurements with estimates from horizontal:vertical spectral ratios

motion broadband seismometers traverses the high-probability, low-power region of the PDFs and is composed of ambient seismic noise. In contrast, PSDs that traverse the highest (>90%) and lowest power (<5%) regions of the PDFs are composed of low-probability transients such as earthquakes and recording system problems (Fig. 2) (McNamara et al., 2009).

After trimming transients, the remaining hourly PSDs are compiled into daily PSD PDFs. Daily PSD PDF medians are computed and used to form daily HVSRs (Fig. 3A). We then compute the average of the daily HVSR estimates to form the weak-motion station HVSR (Sesame European Research Group, 2004). Figure 3B shows the daily HVSR estimates computed from the ratio between the vertical component and the averaged horizontal components. A clear HVSR peak frequency is observed at 3–4 Hz for the portable station GS.SPFD while the HVSR estimate at US.BLA displays no significant ambient noise

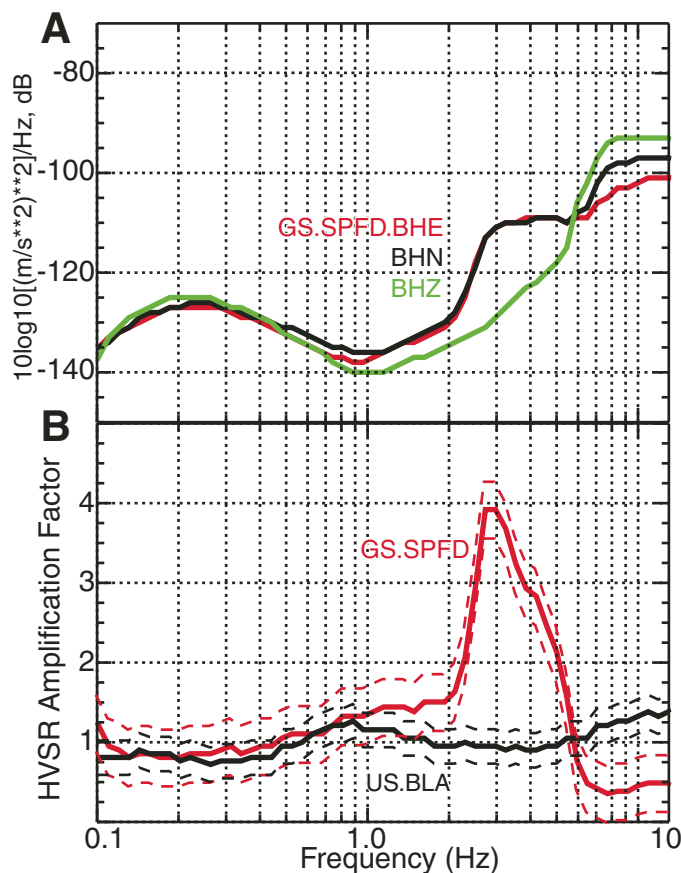


Figure 3. Horizontal:vertical spectral ratio (HVSR) method using portable aftershock station GS.SPFD and Advanced National Seismic System (ANSS) station US.BLA. (A) Power spectral density (PSD) probability density functions (PDF) daily median PSDs for three components of motion that were used to form daily spectral ratios. (B) GS.SPFD HVSR results display a clear resonance peak at 3 Hz with an amplification factor of 4 (red line), whereas the permanent ANSS rock site US.BLA has no clear HVSR peak frequency (black line). Dashed lines show the  $2\sigma$  standard deviation of the daily average HVSR estimate. Double asterisks represent exponent.

resonance frequency peaks. This method was applied to more than 200 weak-motion stations in the eastern United States. Figure 4 shows some of the variability in weak-motion HVSR with peak frequencies in the range of 0.7–8.0 Hz observed at several seismic stations in this study.

A difficulty in estimating HVSR using strong motion sensors is that they are insensitive to low-power ambient noise levels commonly used to compute HVSRs. In order to include strong-motion sensors in this HVSR study we are required to use the low-probability high-power portion of the PSD PDF that is composed of earthquake signals. High-power PSDs observed in the PSD PDFs, such as the 95th percentile, represent the very highest power signals from earthquakes such as the 2011 Mineral earthquake and larger aftershocks. Both weak- and strong-motion instruments were operating at several stations in this study (GS.SPFD, US.BLA, and US.CBN) and make it possible to compare results. Figure 5 shows HVSR estimates formed using daily strong-motion PSD PDF 95th percentiles with average HVSR results computed from the weak motion records. The HVSR peak frequency and amplitude are nearly identical, suggesting that both the median and 95th percentile of the PSD PDF can be used to estimate HVSR.

### HVSR Results

After forming the individual station HVSRs we visually inspect the results for clear peaks and the absence of clear peaks on both the weak and strong motion stations. For stations with clear peaks, we manually pick the peak frequency on the average HVSR estimates and the  $2\sigma$  standard deviations in order to determine the pick uncertainty (Table 1). Stations with no clear

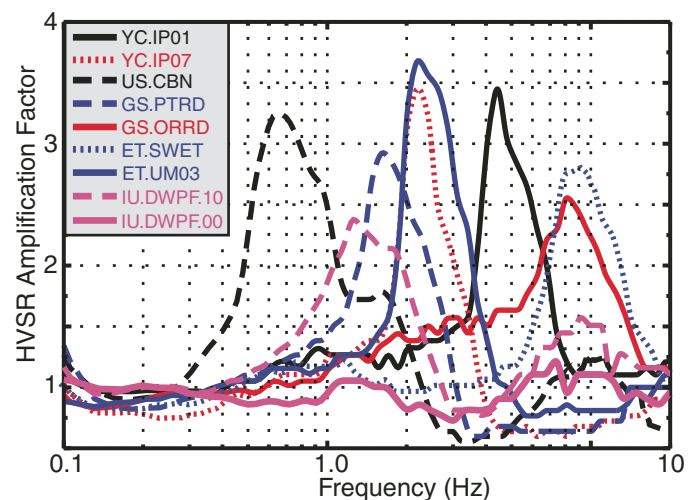


Figure 4. A range of horizontal:vertical spectral ratio (HVSR) results for several seismic stations determined in this study. Across the region we observe a range of resonant frequencies and amplification factors. Also shown is the HVSR comparison at IU.DWPF between surface (IU.DWPF.10) and borehole sensor (IU.DWPF.00).

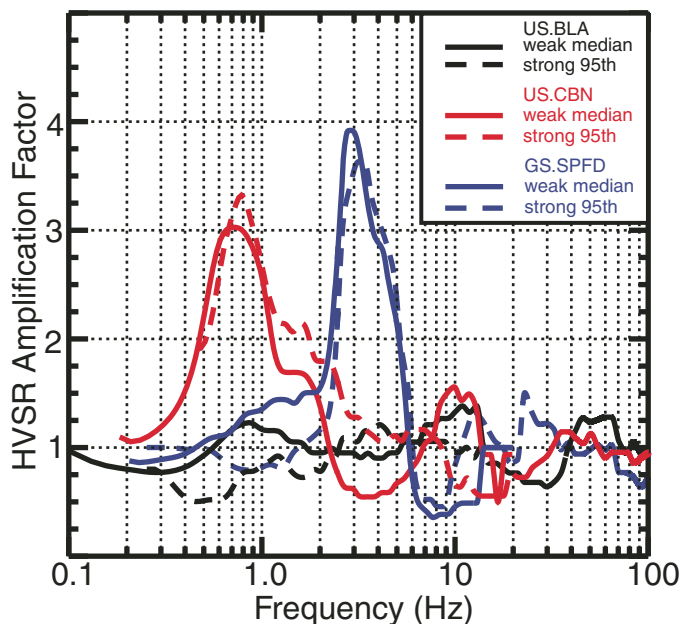


Figure 5. Comparison of colocated weak and strong motion sensors at three different seismic stations (US.CBN, US.BLA, GS.SPFd; see Table 1). The horizontal:vertical spectral ratios (HVSr) computed using both weak motion and strong motion sensors display similar peak frequencies and amplification using colocated sensors.

HVSr peak are considered to have no result (no result [NR]) and are labeled NR in Table 1 (see US.BLA in Figs. 3 and 5).

The results shown in Figures 3–5 demonstrate the variability in HVSr peak frequency and amplification factor observed at several seismic stations in the eastern United States. The resonance frequency ( $f$ ) of a site is related to the thickness ( $h$ ) and the average S-wave velocity ( $V_s$ ) of the softer geologic material near the surface (Lermo and Chavez-Garcia, 1993; Lachet and Bard, 1994; Castellaro and Mulargia, 2009), where  $f = V_s/4h$  (Bard, 1999). For example, US.BLA is installed in a vault excavated into bedrock and shows no significant ambient noise resonance frequency peaks (Table 1; Figs. 1 and 3B). The lack of an HVSr peak indicates that no significant impedance contrast exists below the surface. In contrast, the temporary aftershock station GS.SPFd was installed in a shallow vault in loosely consolidated saprolite and soils (Stolt et al., 1992) and shows a clear HVSr peak at 3 Hz (Fig. 3B). In general, we observe a broad range of resonance peaks, from 0.2 to 10 Hz, with variable width and amplification (Fig. 4).

## DISCUSSION

### Vs30

Understanding the spatial variability of site response is important to hazard mitigation (Boore, 2004). Modern ground-motion prediction equations utilize site amplification factors

TABLE 2. Vs30 OBSERVATIONS AT 66 SEISMIC STATIONS IN THE EASTERN UNITED STATES

Net.Station	Surface Vs30 (m/s)	Topographic Vs30 (m/s)
GS.ORRD	544.0	406.9
GS.SPRD	580.0	356.6
YC.IP01	530.0	450.9
XY.BUPP	483.0	518.9
ET.UOM1	837.0	392.1
NP.9985	382.3	340.4
LD.LD05	461.0	439.1
LD.LD01	507.0	506.3
GS.CVRD	340.0	549.8
ET.UOM2	335.0	354.5
YC.IP02	340.0	316.8
YC.IP05	370.0	457.0
GS.SPFd	464.0	336.3
GS.PTRD	260.0	380.0
YC.IP03	390.0	414.6
YC.IP04	442.0	401.4
AG.WHAR	1190.0	705.1
ET.SWET	840.0	284.7
IU.SSPA	939.0	576.9
NM.CVVA	581.0	244.6
NM.SEAR	984.0	304.8
NM.SIUC	491.0	319.4
NM.UALR	1288	760.0
NQ.NQ793	368.0	356.6
PE.PSUB	551.0	447.9
PN.PPBLN	1077.0	488.5
PN.PPCWF	466.0	310.0
PN.PPMOO	504.0	436.1
PN.PPPCH	429.0	542.7
PN.PPPHS	325.0	244.6
SE.RCRC	519.0	586.7
SE.URVA	528.0	526.9
SE.VWCC	357.0	588.3
US.BLA	700.0	517.3
US.CBN	249.0	206.0
US.GOGA	296.0	709.1
US.LBNH	850.0	760.0
US.LONY	1100	530.2
US.LRAL	568.0	342.6
US.MIAR	1090	311.4
US.MYNC	495.0	760.0
US.NCB	1002	760.0
US.WMOK	1642	558.3
NP.2555	340.0	439.3
US.CBN	279.0	206.0
NP.2511	388.9	285.6
PE.PAGS	525.3	705.2
LD.MVL	671.5	619.6
NP.2648	609.1	571.1
NP.WNC	357.0	612.3
NP.2560	606.8	448.1
XY.JSRW	476.6	263.3
NP.2558	362.0	305.8
XY.URVA	358.9	526.9
GS.LWRD	325.4	263.4
NQ.NQ001	655.4	439.0
NP.2549	497.9	760.0
NP.2405	633.2	321.6
NP.2510	357.5	760.0
US.TZTN	357.5	760.0
NP.2506	431.2	338.9
NP.NAMA	341.5	408.4
NP.CAPTL	334.3	587.9
NQ.NQ957	271.8	285.2
US.CNNC	285.9	598.3
US.MCWV	1483.4	760.0

Note: HVSr—horizontal:vertical spectral ratios; Vs30—shear-wave velocity to a depth of 30 m.

Comparison of Vs30 measurements with estimates from horizontal:vertical spectral ratios

based on broad soil classes that are most commonly defined by the average shear-wave velocity in the upper 30 m (Vs30) (Martin, 1994; Borcherdt, 1994; Wills and Silva, 1998). High Vs30 values are associated with firm, dense rock and lower levels of ground shaking, while lower Vs30 values are associated with softer soils and site amplification of 1.5–2 (Petersen et al., 2008).

Vs30 is commonly computed from surface measurements of Vs using a receiver array and either using active sources or passive ambient noise microtremor sources (Odum et al., 2010, 2013; Stephenson et al., this volume). Following the 2011 Mineral earthquake, Vs30 was measured at the locations of 66 portable and permanent seismic stations in the CVSZ and greater eastern United States (Electric Power Research Institute, 2012; Stephenson et al., this volume; R. Kayen, 2012, personal commun.) (Table 2). This data set of surface Vs30 measurements provides a valuable resource for comparison of proxy methods used to estimate Vs30 and soil class.

In Figure 6 we compare surface measured Vs30 at 21 seismic station locations with clear observations of HVSr peak frequency. A least-squares regression between HVSr peak frequency and Vs30 measured at the surface results in a slope of  $m = 51.90 \pm 65.95$  and intercept of  $b = 254.73 \pm 28.52$  with a data standard deviation = 78.91 m/s (Fig. 6). The relatively low standard deviation and high data cross-correlation coefficient of 0.89

suggests a clear relationship between HVSr peak frequency and surface measurements of Vs30.

Since surface Vs30 measurements are not available at all site locations of interest for earthquake hazard assessment (Petersen et al., 2008), a common method used to estimate Vs30 takes advantage of topographic slope (Allen and Wald, 2007, 2009). For each location of the 66 seismic stations with surface measurements of Vs30 we extract the topographic slope proxy Vs30 from the USGS Global Vs30 Map Server (<http://earthquake.usgs.gov/hazards/apps/vs30/>). As a test, we compare how well our HVSr peak frequency proxy relationship compares with the topographic slope proxy at predicting Vs30 measured at the surface. Figure 7 compares 66 surface measurements of Vs30 to topographic slope proxy Vs30. A least-squares regression results in a slope of  $0.173 \pm 0.065$  and intercept of  $368.79 \pm 42.25$  (data standard deviation = 155.79 m/s, data cross-correlation coefficient = 0.31). The large standard deviation and low cross-correlation coefficient indicates that the topographic slope proxy is not a reliable predictor of Vs30 measured at the surface for this data set. The topographic slope proxy estimate tends to underestimate Vs30 measured at the surface.

In Figure 7 we also determine how well our HVSr peak frequency proxy relationship predicts Vs30 measured at the surface. We estimate Vs30 at 21 seismic stations with clear HVSr

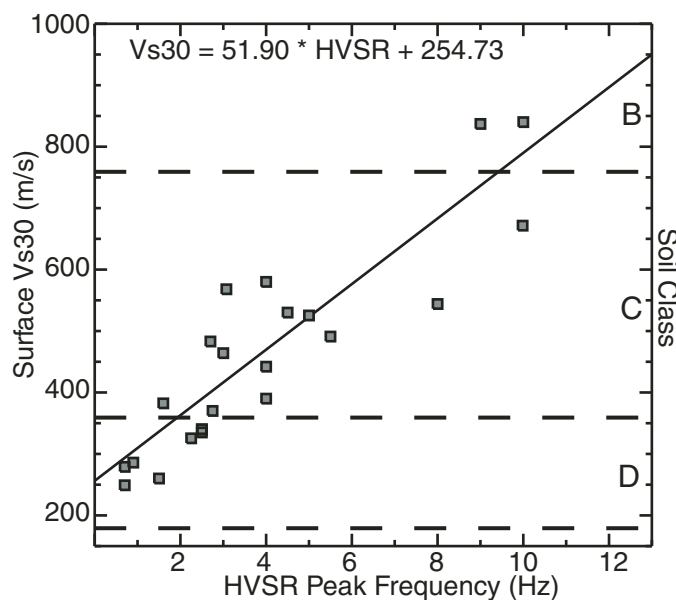


Figure 6. Comparison of Vs30 (shear-wave seismic velocity to 30 m depth; m/s) and horizontal:vertical spectral ratio (HVSr) peak frequency. Squares show results from 21 permanent and portable seismic stations with surface Vs30 measurements and HVSr resonance frequencies determined in this study. Solid line shows the least squares fit to the surface HVSr peak frequency and Vs30 with slope ( $m = 51.90 \pm 65.95$ ) and intercept ( $b = 254.73 \pm 28.52$ ) (data standard deviation = 78.91 m/s, data cross-correlation coefficient = 0.89). Dashed lines delineate Vs30 defined National Earthquake Hazard Reduction Program soil classes.

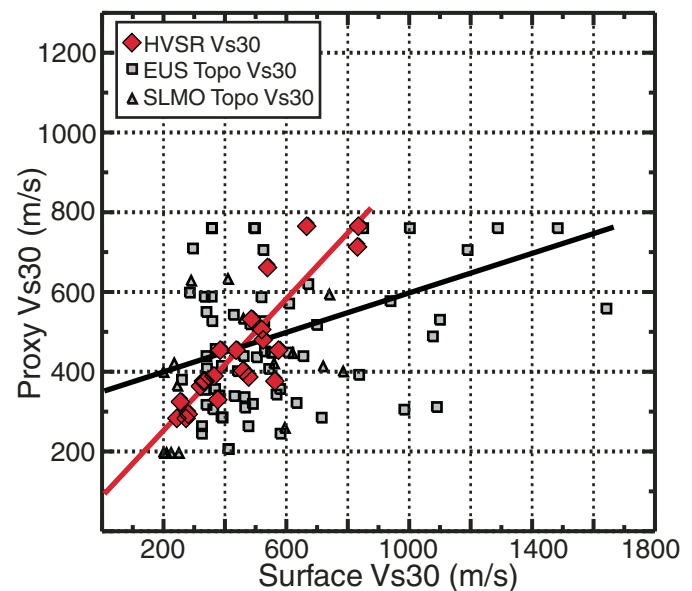


Figure 7. Comparison between topographic slope and surface measured Vs30 (shear-wave seismic velocity to 30 m depth) methods seismic stations in the eastern United States (EUS). A least-squares fit results in a slope of  $0.173 \pm 0.065$  and intercept of  $368.79 \pm 42.25$  (data standard deviation = 155.79 m/s, data cross-correlation coefficient = 0.31; black line). Also shown are Vs30 estimates based on the horizontal:vertical spectral ratio (HVSr) proxy determined in this study (red diamonds). A least-squares fit results in a slope of  $0.783 \pm 0.090$  and intercept of  $99.24 \pm 43.59$  (data standard deviation = 69.76 m/s, data cross-correlation coefficient = 0.89; red line). SLMO—St. Louis, Missouri.

peak frequencies and colocated surface measurements of Vs30. A least-squares fit between surface measured Vs30 and HVSR proxy Vs30 results in a slope of  $m = 0.783 \pm 0.090$  and intercept  $b = 99.24 \pm 43.59$  (data standard deviation = 69.76 m/s, data cross-correlation coefficient = 0.89). The relatively low standard deviation and high data cross-correlation coefficient indicates that HVSR peak frequency can reliably estimate Vs30 measured at the surface for this CVSZ data set.

### Soil Class

The 218 seismic stations used in this study are installed in a broad range of soils and consequently result in a range of HVSR peak frequencies (Figs. 3–5). Figure 6 shows the NEHRP soil class boundaries, defined by Vs30 (Martin, 1994), and the linear relationship observed between HVSR peak frequency and surface measurements of Vs30. If we assume that the empirical linear relationship defines a proxy relationship, we can estimate Vs30 and thereby infer NEHRP soil class for seismic stations with a clear HVSR peak frequency.

In Figure 1 we map the distribution of soil class estimates at 218 seismic stations using the HVSR proxy determined in this study (Table 1). Seismic stations used in this study are located in both solid rock (e.g., US.BLA: <http://earthquake.usgs.gov/monitoring/operations/station.php?network=US&station=BLA>) and in highly weathered and saturated soils such as near the North Anna reservoir and nuclear power plant (GS.ORRD, GS.SPRD) (Fig. 1). We observe that most stations are located in soil classes C (very dense soil and soft rock), CD, and D (stiff soil) (Martin, 1994). Soil class D estimates are most commonly associated with areas of thick sediments such as southeast coastal areas of Virginia, the Carolinas and Florida, the Michigan basin, and Mississippi embayment sediments. Soil class C and HVSR measurements with no clear peak (NR) are common in the higher elevation regions of the Appalachian Mountains. Based on this analysis we see that much of the eastern United States has local site conditions that can significantly amplify ground motions.

The geology of the eastern United States is marked by a wide variety of provinces, from the eastern coastal plains westward to the Appalachian Plateau. The epicentral region of the 2011 Mineral earthquake is located within the Piedmont Province and is characterized by gently rolling topography, deeply weathered bedrock, and a relative paucity of solid rock outcrop. Saprolite is the most common near-surface material in the Piedmont region of Virginia (Stolt *et al.*, 1992), and is generally formed in place as gradationally weathered material from the underlying bedrock. Saprolites are also common in other regions, such as Hong Kong, where strong motion site response studies have shown that thin layers of saprolite (Vs30 = 100–400 m/s) overlying high-velocity bedrock (Vs30 = 1500 m/s) can lead to significant local site amplification (Pappin *et al.*, 2004). In addition, thicker layers of saprolite (~22 m) that overlie very high velocity bedrock (Vs = 2400 m/s) at sites near Mayaguez, Puerto Rico, have been shown to have very large local site amplification (Odum *et al.*, 2013).

Vs30 for saprolite in the 2011 Mineral earthquake epicentral area ranges from 200 to 400 m/s (Stephenson *et al.*, this volume), consistent with soils of classes C and D. Similar to other regions, saprolite with soil classes of C and D within the eastern United States can be expected to produce significant site amplification (Fig. 1).

### Implications for Structures

The characteristics of ground motion that are most important for building design are the duration, amplitude, and frequency of horizontal ground motion. In this study we demonstrate that HVSR peak frequency can be used as a proxy to estimate Vs30 and consequently NEHRP soil class, which are the dominant parameters used to determine local site amplification. The 2011 Mineral earthquake produced shaking sufficient to close the North Anna nuclear power plant, located ~20 km from the epicenter, with reported shaking levels reaching a factor of two times the maximum design limit (Li, 2013; Earthquake Engineering Research Institute, 2011). Recorded peak ground acceleration reached  $2.6 \text{ cm/s}^2$  (Li, 2013; Chapman, 2013) and is consistent with the USGS PAGER intensity model (MMI = VI–VII) (Fig. 1A) and with postevent damage assessment (Earthquake Engineering Research Institute, 2011). As observed in Figure 1A, seismic stations located in the epicentral region of the 2011 Mineral earthquake and near the North Anna Power Station are of soil classes C and D, which can be expected to significantly amplify ground shaking (Petersen *et al.*, 2008).

Also of great importance in building design is the frequency of horizontal ground motion. When the frequency content of ground motion is near a building's natural frequency, the building and the ground motion are in resonance with one another. Based on the conventional relationship in which the resonance period ( $1/f$ ) is  $0.1 \times$  number of stories, we can estimate building heights that are most sensitive to the resonance frequency of the soils in this study. For example, a 20-story building is likely most sensitive to soils with resonant frequency of 0.5 Hz (2.0 s period), similar to the observation at US.CBN (Fig. 4), whereas a 10-story building is sensitive to soils with a resonant frequency of 1.0 Hz (1 s period), similar to stations near the North Anna Power Station (Table 1). The highest HVSR peak frequencies observed for soils in this study (ET.SWET, GS.OORD; ~10 Hz) suggest that single-story buildings are also at risk. The wide range of resonant frequency observations is consistent with the broad range of building damage observed in the epicentral region immediately following the mainshock (Earthquake Engineering Research Institute, 2011).

### Limitations and Uncertainty

Though the distribution of our soil class estimates is generally consistent with regional geology, individual station results can be difficult to interpret. This is the case for stations labeled NR that do not have a clear peak frequency. If a seismic station

*Comparison of Vs30 measurements with estimates from horizontal:vertical spectral ratios*

is part of a permanent seismic network, most likely the station is not sensitive to the local shallow soil. Most permanent earthquake monitoring stations are built to reduce noise by placing sensors on concrete piers coupled directly to bedrock or in borehole installations (McNamara et al., 2009). As demonstrated with IU.DWPF in Figure 4, deeply buried sensors do not record site effects because they are below the shallow soils. Based on the peak HVSR resonance frequency observed with the surface sensor at IU.DWPF.10 (1 Hz), the surface soils should have a Vs30 = 316 m/s and soil class D (Fig. 6). In contrast, the borehole sensor (IU.DWPF.00) has no HVSR peak frequency because it is coupled to solid rock at depth of 162 m (Fig. 4). Many of the permanent ANSS, GSN (Global Seismographic Network), and USArray TA (transportable array) stations have no HVSR peak frequency (Table 1; Fig. 1B). Sensors buried at shallow depth, such as those used in portable or temporary aftershock networks, are often better for determining high-frequency soil characteristics. This contrasts with the permanent ANSS station US.CBN, which has a clearly observed HVSR peak frequency of ~0.7 Hz (Fig. 4) due to installation in thick class D soil (Table 1; R. Kayen, 2012, personal commun.) (<http://earthquake.usgs.gov/monitoring/operations/station.php?network=US&station=CBN>). Based on the regression results shown in Figure 6, we estimate that Vs30 = 302 m/s.

Because the paucity of local observations limits our ability to adequately evaluate near-field strong ground motion, we require proxy methods to estimate site response for most locations. It is possible that the linear relationship between Vs30 and HVSR peak frequency, determined in this study, is unique to the 21 stations located in the CVSZ and may not be an appropriate Vs30 proxy for the entire eastern United States and other regions. Therefore we recommend that results from this study be compared to different regions where surface Vs30 measurements are available for existing seismic stations. Since surface measurements of Vs30 are spatially limited, we also recommend additional measurement of Vs30 at existing seismic stations.

## CONCLUSIONS

In this study, we compute HVSR peak frequency for 218 seismic stations in the eastern United States. The surface measured Vs30 data set collected after the 2011 Mineral, Virginia, earthquake provides an opportunity to compare these observations with the HVSR results at the same locations. We show a strong linear relationship between HVSR peak frequency and surface Vs30 measurements in the CVSZ and suggest that this approach can be used as a proxy to estimate Vs30 and NEHRP soil class in the eastern United States. For stations in this study, the HVSR Vs30 proxy is more reliable at predicting surface measured Vs30 than the topographic slope proxy. Because surface measurements of Vs30 are spatially limited, we suggest that our approach can be used where seismic stations are available in order to calibrate topographic slope estimates of Vs30 that are commonly used to estimate shaking hazard. Local soil class is a

significant issue for the construction of buildings and other structures, and is commonly used by engineers in the development of building design criteria. Based on our results it is important to quantify local soil class in order to provide guidance on the design of buildings and infrastructure in regions that can experience strong ground shaking. Studies of this nature are also relevant to rapid USGS earthquake assessment and hazard products that are important for the improvement of building codes in the eastern United States.

## ACKNOWLEDGMENTS

Data used in this study were recorded at regional broadband stations operated by the U.S. Geological Survey (USGS), regional ANSS (Advanced National Seismic System) networks and the IRIS (Incorporated Research Institutions for Seismology) transportable array. In addition, 47 portable stations were deployed shortly after the main shock. Station location information, instrument response transfer functions, and waveform data for all portable and permanent seismic stations used in this study are archived and available for download from the IRIS Data Management Center. Analysis and mapping software used includes PQLX (McNamara and Boaz, 2010), SAC (Goldstein et al., 2003; Goldstein and Snoke, 2005), GMT (Wessel and Smith, 1991, 2004) and Matlab.

We greatly appreciate the rapid response and hard work of the aftershock deployment field crew. The crew included Anne Meltzer, Steve Horton, Mitch Withers, Patrick Bastion, Noel Barstow, and additional staff from the USGS and IRIS PASSCAL (Program for Array Seismic Studies of the Continental Lithosphere). Field support for the IRIS PASSCAL stations was provided by National Science Foundation grant EAR-1148357 to Lehigh University. We also thank staff at the USGS National Earthquake Information Center (A. Leeds, J. Allen, M. Meremonte), IRIS PASSCAL, UNAVCO, and station hosts in Louisa County, Virginia, for material and logistical support. We thank T. Pratt and A. Frankel for helpful discussions on the relationship between site response and earthquake hazard in the eastern United States and W. Horton and A. Shah for discussions on regional geology in the eastern United States. Thoughtful comments were provided by Paul Bodin and one anonymous reviewer. Any use of trade, product, or firm names is for descriptive purposes only and does not imply endorsement by the U.S. Government.

## REFERENCES CITED

- Algermissen, S.T., and Perkins, D.M., 1976, A Probabilistic Estimate of Maximum Acceleration in Rock in the Contiguous United States: U.S. Geological Survey Open-File Report 76-416, 45 p.
- Allen, T.I., and Wald, D.J., 2007, Topographic Slope as a Proxy for Seismic Site Conditions ( $V_s^{30}$ ) and Amplification around the Globe: U.S. Geological Survey Open-File Report 2007-1357, 69 p.
- Allen, T.I., and Wald, D.J., 2009, On the use of high-resolution topographic data as a proxy for seismic site conditions (VS30): *Seismological Society of America Bulletin*, v. 99, p. 935–943, doi:10.1785/0120080255.

- Bard, P.Y., 1999, Micro tremor measurements: A tool for site effect estimation?, *in* Irikura, K., Kudo, K., Okada, H., and Satasini, T., eds., Proceedings of the Second International Symposium on Effect of Surface Geology on Seismic Motion (Yokohama, Japan): Rotterdam, Balkema, p. 1251–1279.
- Benz, H., Frankel, A., and Boore, D., 1997, Regional Lg attenuation for the continental United States: *Seismological Society of America Bulletin*, v. 87, p. 606–619.
- Bodin, P., and Horton, S., 1999, Broadband microtremor observation of basin resonance in the Mississippi embayment, central US: *Geophysical Research Letters*, v. 26, p. 903–906, doi:10.1029/1999GL900146.
- Bollinger, G.A., 1969, Seismicity of the central Appalachian states of Virginia, West Virginia, and Maryland—1758 through 1968: *Seismological Society of America Bulletin*, v. 59, p. 2103–2111.
- Boore, D., 2004, Can site response be predicted?: *Journal of Earthquake Engineering*, v. 8, Special Issue 1, p. 1–41.
- Borcherdt, R.D., 1994, Estimates of site-dependent response spectra for design (methodology and justification): *Earthquake Spectra*, v. 10, p. 617–653, doi:10.1193/1.1585791.
- Borcherdt, R.D., and Gibbs, J.F., 1976, Effects of local geological conditions in the San Francisco Bay region on ground motions and the intensities of the 1906 earthquake: *Seismological Society of America Bulletin*, v. 66, p. 467–500.
- Building Seismic Safety Council, 2009, NEHRP Recommended Seismic Provisions for New Buildings and Other Structures: Washington, D.C., Federal Emergency Management Agency, FEMA P-750, 406 p.
- Castellaro, S., and Mulargia, F., 2009, Vs30 estimates using constrained H/V measurements: *Seismological Society of America Bulletin*, v. 99, p. 761–773, doi:10.1785/0120080179.
- Chapman, M.C., 2005, The seismicity of central Virginia: *Seismological Research Letters*, v. 76, p. 115.
- Chapman, M.C., 2013, On the rupture process of the 23 August 2011 Virginia earthquake: *Seismological Society of America Bulletin*, v. 103, p. 613–628, doi:10.1785/0120120229.
- Edwards, E., Michel, C., Poggi, V., and Fah, D., 2013, Determination of site amplification from regional seismicity: Application to the Swiss National Seismic Networks: *Seismological Research Letters*, v. 84, p. 611–621, doi:10.1785/0220120176.
- Earthquake Engineering Research Institute, 2011, Learning from earthquakes: The M<sub>w</sub> 5.8 Virginia earthquake of August 23, 2011: Earthquake Engineering Research Institute Special Earthquake Report, <http://www.eqclearinghouse.org/2011-08-23-virginia/files/2011/12/EERI-GEER-DRC-Virginia-eq-report.pdf>, 13 p.
- Electric Power Research Institute, 2012, EPRI (2004, 2006) Ground-motion model (GMM) review project: Shear wave velocity measurements at seismic recording stations: Electric Power Research Institute Technical Report EP-P43952/C19088.
- Field, E.H., and Jacob, K.H., 1995, A comparison and test of various site-response estimation techniques, including three that are not reference-site dependent: *Seismological Society of America Bulletin*, v. 85, p. 1127–1143.
- Frankel, A., Mueller, C., Barnhard, T., Perkins, D., Leyendecker, E., Dickman, N., Hanson, S., and Hopper, M., 1996, National Seismic-Hazard Maps: Documentation June 1996: U.S. Geological Survey Open-File Report 96-532, 110 p.
- Goldstein, P., and Snoke, A., 2005, SAC availability for the IRIS community: DMS Electronic Newsletter 7, no.1.
- Goldstein, P., Dodge, D., Firpo, M., and Minner, L., 2003, “SAC2000: Signal processing and analysis tools for seismologists and engineers, *in* Lee, W.H.K., Kanamori, H., Jennings, P.C., and Kisslinger, C., eds., The IASPEI International Handbook of Earthquake and Engineering Seismology: London, Academic Press, 1000 p.
- Hartzell, S., Meremonte, M., Ramirez-Guzman, L., and McNamara, D.E., 2014, Ground motion in the presence of complex topography: Earthquake and ambient noise sources: *Seismological Society of America Bulletin*, v. 104, p. 451–466, doi:10.1785/0120130088.
- Hough, S., 2012, Initial assessment of the intensity distribution of the 2011 Mw5.8 Mineral, Virginia earthquake: *Seismological Research Letters*, v. 83, p. 649–657, doi:10.1785/0220110140.
- Lachet, C., and Bard, P.Y., 1994, Numerical and theoretical investigations on the possibilities and limitation of Nakamura's technique: *Journal of Physics of the Earth*, v. 42, p. 377–397, doi:10.4294/jpe1952.42.377.
- Lermo, J., and Chavez-Garcia, F.J., 1993, Site effect evaluation using spectral ratios with only one station: *Seismological Society of America Bulletin*, v. 83, p. 1574–1594.
- Li, Y., 2013, Post 23 August 2011 Mineral, Virginia, earthquake investigations at North Anna Nuclear Power Plant: *Seismological Research Letters*, v. 84, p. 468–473, doi:10.1785/0220120179.
- Martin, G.R., ed., 1994, Proceedings, NCEER/SEAOC/BSSC Workshop on Site Response during Earthquakes and Seismic Code Provisions, University of Southern California, November 18–20, 1992: Buffalo, New York, National Center for Earthquake Engineering Research Special Publication NCEER-94-SP01.
- McNamara, D., and Buland, R., 2004, Ambient noise levels in the continental United States: *Seismological Society of America Bulletin*, v. 94, p. 1517–1527, doi:10.1785/012003001.
- McNamara, D.E., and Boaz, R.I., 2010, PQLX: A Seismic Data Quality Control System Description, Applications and Users Manual: U.S. Geological Survey Open-File Report 2010-1292, 41 p.
- McNamara, D.E., Hutt, C.R., Gee, L.S., Benz, H.M., and Buland, R.P., 2009, A method to establish seismic noise baselines for automated station assessment: *Seismological Research Letters*, v. 80, p. 628–637, doi:10.1785/gssrl.80.4.628.
- McNamara, D.E., Benz, H.M., Herrmann, R.B., Bergman, E.A., and Chapman, M.C., 2014a, The Mw 5.8 Central Virginia seismic zone earthquake sequence of August 23, 2011: Constraints on earthquake zone parameters and fault geometry: *Seismological Society of America Bulletin*, v. 104, p. 40–54, doi:10.1785/0120130058.
- McNamara, D.E., Gee, L., Benz, H., and Chapman, M., 2014b, Frequency dependent seismic attenuation in the eastern US as observed from the 2011 central Virginia earthquake and aftershock sequence: *Seismological Society of America Bulletin*, v. 104, p. 55–72, doi:10.1785/0120130045.
- Mundepi, A.K., Lindholm, C., and Kamal, 2009, Soft soil mapping using horizontal to vertical spectral ratio (HVSR) for seismic hazard assessment of Chandigarh city in Himalayan foothills, north India: *Geological Society of India Journal*, v. 74, p. 551–558, doi:10.1007/s12594-009-0166-x.
- Nakamura, Y., 1989, A method for dynamic characteristics estimation of sub-surface using microtremor on the surface: *Railway Technical Research Institute Report*, v. 30, p. 25–33.
- Odum, J.K., Stephenson, W.J., and Williams, R.A., 2010, Predicted and observed spectral response from co-located shallow, active and passive source Vs data at five ANSS sites, Illinois and Indiana, USA: *Seismological Research Letters*, v. 81, p. 955–964, doi:10.1785/gssrl.81.6.955.
- Odum, J.K., Stephenson, W.J., Williams, R.A., and von Hillebrandt-Andrade, C., 2013, Vs30 and spectral response from collocated shallow, active and passive-source Vs data at 27 sites in Puerto Rico: *Seismological Society of America Bulletin*, v. 103, p. 2709–2728, doi:10.1785/0120120349.
- Pappin, J.W., Free, M.W., Bird, J., and Koo, R., 2004, Evaluation of site effects in a moderate seismicity region, Hong Kong, *in* Canadian Association for Earthquake Engineering, International Association for Earthquake Engineering, 13th World Conference on Earthquake Engineering, Vancouver, B.C., Canada, August 2004, Technical Programme and Handbook: Vancouver, British Columbia, 13WCEE.
- Petersen, M.D., Frankel, A.D., Harmsen, S.C., Mueller, C.S., Haller, K.M., Wheeler, R.L., Wesson, R.L., Zeng, Y., Boyd, O.S., Perkins, D.M., Luco, N., Field, E.H., Wills, C.J., and Rukstales, K.S., 2008, Documentation for the 2008 Update of the United States National Seismic Hazard Maps: U.S. Geological Survey Open-File Report 2008-1128, 61 p.
- Peterson, J., 1993, Observation and Modeling of Seismic Background Noise: U.S. Geological Survey Technical Report 93-322, 95 p.
- Pratt, T.L., and Brocher, T.M., 2006, Site response and attenuation in the Puget lowland, Washington State: *Seismological Society of America Bulletin*, v. 96, p. 536–552, doi:10.1785/0120040200.
- SESAME European Research Group, 2004, Guidelines for the Implementation of the H/V Spectral Ratio Technique on Ambient Vibrations: Measurements, Processing and Interpretation: SESAME European Project EVG1-CT-2000-00026, 62 p., <http://sesame-fp5.obs.ujf-grenoble.fr/index.htm>.
- Stephenson, W.J., Odum, J.K., McNamara, D.E., Williams, R.A., and Angster, S.J., 2015, this volume, Ground-motion site effects from multimethod shear-wave velocity characterization at 16 seismograph stations deployed for aftershocks of the August 2011 Mineral, Virginia, earthquake, *in* Horton, J.W., Jr., Chapman, M.C., and Green, R.A., eds., The 2011 Mineral, Virginia, Earthquake, and Its Significance for Seismic Hazards in Eastern

*Comparison of Vs30 measurements with estimates from horizontal:vertical spectral ratios*

- North America: Geological Society of America Special Paper 509, doi:10.1130/2015.2509(03).
- Stolt, M.H., Baker, J.C., and Simpson, T.W., 1992, Characterization and genesis of saprolite derived from gneissic rocks of Virginia: *Soil Science Society of America Journal*, v. 56, p. 531–539, doi:10.2136/sssaj1992.03615995005600020030x.
- Toshinawa, T., Hisada, Y., Konno, K., Shibayama, A., Honkawa, Y., and Ono, H., 2004, Topographic site response at a Quaternary terrace in Hachioji, Japan, observed in strong motions and microtremors, *in* Canadian Association for Earthquake Engineering, International Association for Earthquake Engineering, 13th World Conference on Earthquake Engineering, Vancouver, B.C., Canada, August 2004, Technical Programme and Handbook: Vancouver, British Columbia, 13WCEE.
- Wald, D.J., Jaiswal, K.S., Marano, K.D., Bausch, D.B., and Hearne, M.G., 2010, PAGER—Rapid assessment of an earthquake’s impact: U.S. Geological Survey Fact Sheet 2010-3036, 4 p.
- Wessel, P., and Smith, W., 1991, Free software helps display data: *Eos* (Transactions, American Geophysical Union), v. 72, p. 441–446, doi:10.1029/90EO00319.
- Wessel, P., and Smith, W.H.F., 2004, The Generic Mapping Tools (GMT) version 4 technical reference and cookbook: Manoa, University of Hawaii School of Ocean and Earth Science and Technology, 251 p., [http://www.soest.hawaii.edu/gmt/gmt/pdf/GMT\\_Docs.pdf](http://www.soest.hawaii.edu/gmt/gmt/pdf/GMT_Docs.pdf).
- Wills, C.J., and Silva, W., 1998, Shear wave velocity characteristics of geologic units in California: *Earthquake Spectra*, v. 14, p. 533–556, doi:10.1193/1.1586014.

MANUSCRIPT ACCEPTED BY THE SOCIETY 6 JUNE 2014

